ELSEVIER

Sensors and Actuators B 23 (1995) 41–47

SENSORS AND ACTUATORS B CHEMICAL

Microfabricated heavy metal ion sensor

Gregory T.A. Kovacs [a,*], Christopher W. Storment [a], Samuel P. Kounaves [b]

[a] *Department of Electrical Engineering, Stanford University, Center for Integrated Systems, Room CIS 130, M/C 4070, Stanford, CA 94305, USA*

[b] *Department of Chemistry, Tufts University, Medford, MA 02155, USA*

Received 7 December 1993; in revised form 21 July 1994; accepted 2 August 1994

Abstract

A novel microfabricated electrochemical sensor has been developed for the detection and measurement of heavy metal ions in aqueous media. The sensor consists of a silicon substrate, on which is fabricated an electrically interconnected, but diffusionally isolated, array of thin-film iridium microelectrodes upon which a thin film of mercury is electrodeposited. Square-wave anodic-stripping voltammetry is used for quantitative analysis. This method involves an initial preconcentration phase in which the array is held at a cathodic potential such that the metal ions are reduced and amalgamated into the mercury, followed by anodic stripping (re-oxidation) of the metal ions. The charge required to strip a given ionic species completely is proportional to its initial concentration in the test solution. Sensitivity in the parts per billion range has been demonstrated without the addition of supporting electrolytes, deoxygenation, agitation, or any other alterations to the water samples.

Keywords: Electrochemical sensor; Heavy metal ion sensor; Microfabrication

1. Introduction

We present a novel microfabricated sensor for the analysis of aqueous media to determine their content of heavy metals, such as lead, cadmium, and the like. An electrochemical technique, anodic-stripping voltammetry (ASV) is used for the analyses (discussed further below) [1]. In its most general form, the ASV technique involves the use of an electrode consisting of an underlying metal layer upon which a small quantity of mercury is electrodeposited. When making measurements, the electrode is first held at a cathodic potential so that heavy metal ions from the solution are reduced (plated) at the surface of the mercury and are dissolved within it, serving as a 'preconcentration' step to increase their concentration greatly within the mercury. After a period of time, the voltage applied to the electrode is scanned in the anodic direction to reoxidize the metals dissolved in the mercury and the resulting currents are measured. As the potential approaches the value at which each metal reoxidizes, current begins to flow, eventually reaching a peak. As the applied potential is further increased, depletion of the electroactive reactants and the formation of a concentration gradient leads to a decrease in current. If multiple electroactive species are present, several peaks will be seen superimposed on a rising baseline current as the potential is shifted cathodically. The current peaks thus obtained correspond to the complete oxidation of each metal species from the mercury. By determining the total charge or peak current corresponding to each peak, the concentration of each metal ion in the test solution can be computed (typically using pre-calibration or serial additions of known reference concentrations). This technique is very sensitive and useful in applications such as trace heavy metal concentration measurements in water and soil, as well as general applications in analytical and clinical chemistry and other fields.

In general, voltammetry is carried out by applying a potential that is varied linearly with time to the working electrode (relative to a reference electrode). The idea behind square-wave voltammetry (SWV) [2] is to perturb the linear ramp voltage rapidly by superimposing a higher-frequency square wave, as illustrated in Fig. 1. The advantages of this approach derive from the facts that the Faradaic current can be isolated from the electrode charging currents and that the rapid perturbations of the electrode prevent the diffusion layer from extending far away from the electrode. Overall, SWV has significant advantages over simple

* Corresponding author.

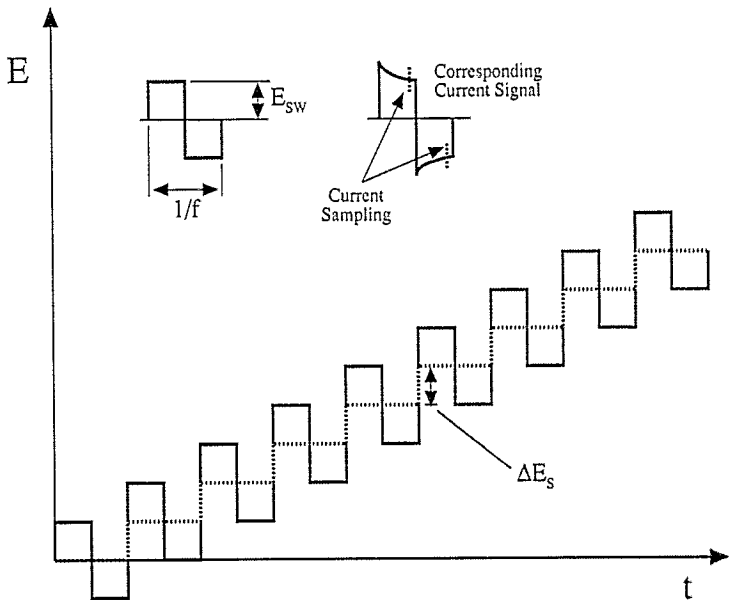

Fig. 1. Example waveforms used in square-wave anodic-stripping voltammetry. A square wave of amplitude E_{sw} is superimposed on a staircase waveform of step height ΔE_S. The resulting potential is applied to the working electrode via a potentiostat and the current is sampled at the ends of both the cathodic and anodic phases of each square-wave cycle.

voltammetry, providing a net increase in sensitivity and decreased analysis times.

When a square-wave voltage is applied, current flows as a result of the Faradaic reaction (providing the signal of interest) and to charge the double-layer capacitance of the electrode. The capacitive current, i_C, decays exponentially as a function (to first order) of the electrode capacitance (on the order of 0.1–1 pF μm^{-2}) in series with the solution resistance. For a step potential change ΔE, i_C is given by

$$i_C = \frac{\Delta E}{R} \exp[-t/RC] \quad (1)$$

where R is the solution resistance (Ω) and C is the electrode capacitance (F). The capacitance of an electrode is (for smooth electrodes) directly proportional to area, and therefore i_C is exponentially related to the electrode area.

The Faradaic current, i_F, which decays more slowly, is given for a hemispherical microelectrode by

$$i_F = nFADC_\infty \left[\frac{1}{(\pi Dt)^{1/2}} + \frac{1}{r_0} \right] \quad (2)$$

where n is the number of electrons transferred, F is 9.6485×10^4 C mol^{-1}, A is the electrode area (m^2), D is the diffusion coefficient of the species of interest (m^2 s^{-1}), C_∞ is the bulk concentration of the species under consideration (mol m^{-3}) and r_0 is the radius of the hemisphere (m).

Therefore, i_F can be measured after a suitable time has elapsed for the decay of i_C. In SWV, i_F is measured at the end of both the cathodic and anodic phases of each square wave, as indicated in Fig. 1. By subtracting these measured currents, the net reaction current can be directly obtained. Square-wave anodic-stripping voltammetry (SWASV) is the combination of the SWV technique with the previously mentioned cathodic preconcentration of the species of interest in (or on) the electrode.

It can be seen from Eqs. (1) and (2) that the ratio of Faradaic to capacitive current increases with decreasing electrode area. Aside from electronic and external noise, this is a key determinant of the net signal-to-noise ratio (SNR), illustrating the principal advantage of using microelectrodes. In addition, the use of microelectrodes involves higher signal currents than for larger electrodes due to the enhanced diffusion of electroactive species. By designing an array of electrically connected microelectrodes spaced far enough apart on a substrate to guarantee non-overlapping diffusion fields, each microelectrode maintains a spherical diffusion layer and thus a large mass-transport capability (larger signal currents). In addition, the size of the current peaks seen during stripping can be increased independently of the electronic noise floor by increasing the predeposition time (up to the solid solubility limits of the metals in mercury). This allows for the modulation of the sensitivity of the sensor by simple modification of the operational parameters.

Another issue that determines the net SNR of the measurements is the fact that the reduction of dissolved oxygen in the test solution occurs over the potential range of interest. This leads to localized pH changes and a large current, which can be a complex function of time and potential and may interfere with the signal current. The effects of the oxygen reduction can be mitigated by using SWASV and further reduced by

subtracting the oxygen-reduction background current from the data [3]. The procedure involves carrying out the anodic stripping, allowing the working electrode to float electrically for a short time (typically a few seconds) for diffusion of oxidation products away from it, and then repeating the stripping potentials on the now-depleted electrode to measure the oxygen-reduction background current. The background current is then numerically subtracted from the stripping current.

Another critical determinant of performance is the choice of metal underlying the mercury of the ASV electrodes. Mercury forms amalgams with most metals suitable as electrodes, but its solubility in iridium is well below 10^{-6} wt.% [4,5]. Thus neither dissolution of the iridium nor intermetallic compound formation between the iridium and mercury occurs. In addition, it has been shown that the Hg–solution surface tension in relation to Hg–Ir surface energy inherently favors the formation of a stable well-adhering mercury hemisphere on iridium disks with diameters on the order of a few microns [6]. Previously published work has described the fabrication and characterization of single Ir-based mercury electrodes using commercially available iridium wires (by sealing etched iridium wire in a glass capillary or other insulating sleeve and polishing a cleaved end) [7].

Previous authors have described both photolithographically or manually fabricated arrays of microelectrodes [8–10], taking advantage of their increased SNR. Thin-film iridium microelectrodes for use as interfaces to nervous tissue have been fabricated at Stanford [11] and the University of Michigan [12]. This work represents the first microfabricated thin-film iridium microelectrode arrays specifically designed for electrochemical analysis.

Since the patterns of these microelectrodes are defined photolithographically, it is just as easy to fabricate large arrays as single ones. The smaller dimensions attainable in this way offer superior performance and repeatability. This approach also provides the capability to mass-produce microelectrodes in 'arrays of arrays' such that one or more elements of an array can be used at a given time to make electrochemical measurements, while the remainder can be used at a later time. In addition, the high-accuracy photolithographic processes used in their fabrication help assure reproducibility of array geometries from device to device (extremely difficult with manually fabricated electrodes, such as drawn wires).

The use of silicon substrates has the additional advantage of providing for future integration of on-chip microelectronic circuits such as potentiostats. Even without monolithic integration, the combination of a sensor of this type, an integrated potentiostat chip, and a single-chip microcontroller will lead to a complete electroanalytical system in less than a cubic centimeter of volume. The overall goal of this work is to develop such low-cost 'intelligent' sensor modules for environmental and analytical chemistry, clinical and consumer applications.

2. Fabrication

The fabrication process, as illustrated by a cross section of a completed device in Fig. 2, is begun by thermally oxidizing a 100 mm silicon wafer to a thickness of 0.5 μm. The 'wet' oxide growth is carried out at a temperature of 1100 °C for 45 min. On this insulating layer of silicon dioxide the iridium microelectrodes are then deposited and patterned at the same time using a sputter lift-off process. The technique begins with the deposition of a 0.5 μm thick layer of Al (or any other suitable material that etches quickly and whose etchant will not attack the metal that is to be deposited and patterned). Standard photoresist is applied and patterned to define the microelectrodes, and subjected to a deep ultraviolet cure and a 150 °C post-bake so that it can withstand the sputter deposition environment. The Al undercut layer is then wet etched (using a phosphoric acid-based etchant) so that the top layer of photoresist is undercut by 1–2 μm. This overhanging lip of photoresist prevents the sputtered metal from coating the sidewalls during deposition and thus leaves an access path for the stripper solvent to follow during the dissolution step that removes the unwanted metal above the photoresist layer. A 30 nm Ti adhesion layer

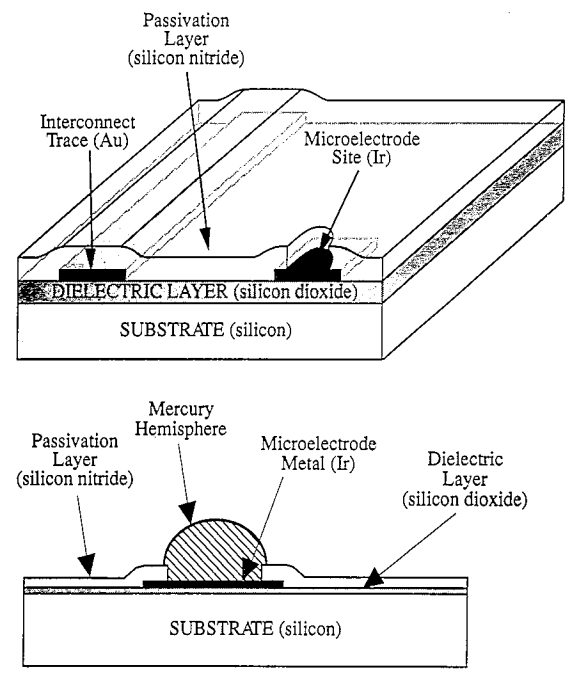

Fig. 2. Illustration of the cross section of a completed microelectrode device showing the relationships of the different layers (top) and the approximate form of the electrodeposited mercury hemisphere (bottom).

and then a 300 nm Ir layer are deposited using d.c. magnetron sputtering, the resist and unwanted metal are removed, and the undercut Al layer is removed by wet etching.

Once the iridium microelectrodes are deposited, a 0.5 μm gold interconnect and bond-pad layer is lift-off deposited and patterned using Si as the undercut layer rather than Al, due to its better adhesion to Ir. This substitution also requires the use of isotropic plasma etching (using CF_4 and O_2 reactant gases) instead of wet etching to form an undercut structure with the Si, since all wet Si etches will attack the Ti adhesion layer beneath the Ir. A 30 nm Ti layer and then a 500 nm Au layer are then deposited by electron-beam evaporation. This is followed by an acetone spray to lift off unwanted metal and plasma etching to remove the silicon (using SF_6 and C_2ClF_5 reactant gases).

Next, a silicon nitride insulating layer is deposited by a plasma-enhanced chemical vapor deposition (PECVD) process to a thickness of 0.5 or 1.0 μm, from SiH_4 (2% in N_2 diluent) and NH_3 reactant gases. Since this deposition is carried out at 300 °C, it is compatible with the inclusion of active microelectronic circuits in the future (as opposed to other CVD silicon nitride processes, which require considerably higher temperatures, on the order of 700 °C). This layer serves to isolate the underlying metal traces from the external environment both electrically and chemically. Via holes through the silicon nitride layer are selectively plasma etched (using SF_6 and C_2ClF_5 reactant gases) to expose the microelectrodes and the bond pads. The individual devices are then separated by conventional wafer dicing, cleaned, inspected, and sorted.

Custom-designed printed circuit board carriers were fabricated commercially. Individual microelectrode devices are mounted on a circuit board using cyanoacrylate adhesive, and gold bond wires are connected between the silicon device and gold-plated circuit board traces on the carrier. The bond wires are then over-potted with Epo-Tek K/5022-87DT two-part epoxy (Epoxy Technology, Inc., Billerica, MA) to protect them from mechanical and chemical damage.

3. Design

A primary objective for these devices is the ability to use arrays of microelectrodes electrically in parallel but with isolated diffusion fields for each site. Initial work was carried out using an array of 16 individually-addressable Ir microelectrodes with diameters of 20 μm at center-to-center spacings of 45 μm in two lines of eight elements, separated by 375 μm. A scanning electron micrograph (SEM) of one of these arrays is shown in Fig. 3.

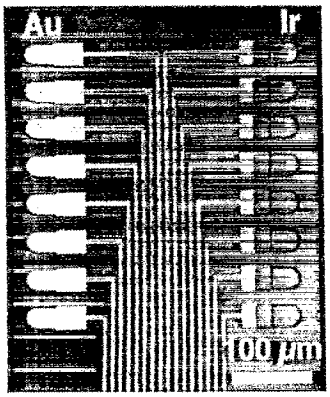

Fig. 3. Optical micrograph of the type of microelectrode array with individually addressable electrodes used for determination of the minimum spacing of the array elements. The microelectrodes shown on the right are iridium and those on the left are gold (not used in this work). The arrays used had uniform 20 μm diameter electrodes.

Using these devices, it was estimated that non-overlapping diffusion fields could be achieved (for the electrochemical parameters used in this work, typically $f=120$ Hz, $E_{sw}=25$ mV, $\Delta E_s=5$ mV) with inter-electrode spacings of approximately 100 μm [13]. This was demonstrated using chronocoulometric techniques, as well as verification that the 1 μm recess above the Ir surfaces did not interfere with electrochemical response. In addition, in the same work, the fact that the microlithographically fabricated Ir microelectrode array exhibits electrochemical behavior as predicted by hemispherical Hg microelectrode theory was demonstrated.

The devices used for the SWASV experiments were designed using this information and consist of 19 electrically interconnected Ir microelectrodes measuring 10 μm in diameter and spaced 300 μm center-to-center to nearest neighbors. Inter-electrode electrical connections are made using a 'skeleton' of 30 μm iridium traces to minimize parasitic capacitances relative to a solid iridium disk. The design trade-off inherent in this approach, however, is that the resistance of the iridium traces interconnecting the microelectrodes increases as their width is decreased. The trace widths could readily be decreased without undue resistive effects in future designs. SEM views of the entire array, as well as an individual microelectrode site, are shown in Fig. 4.

4. Electrochemical methods

SWASV was carried out with a model 273 potentiostat/galvanostat (EG&G PAR, Princeton, NJ) interfaced to a DEC p420-SX (IBM™ compatible) microcomputer and using EG&G model 270 software. A two-electrode system was employed, with a custom-fabricated solid-state Nafion™-coated Ag/AgCl reference electrode employed to avoid introduction of electrolyte by the ref-

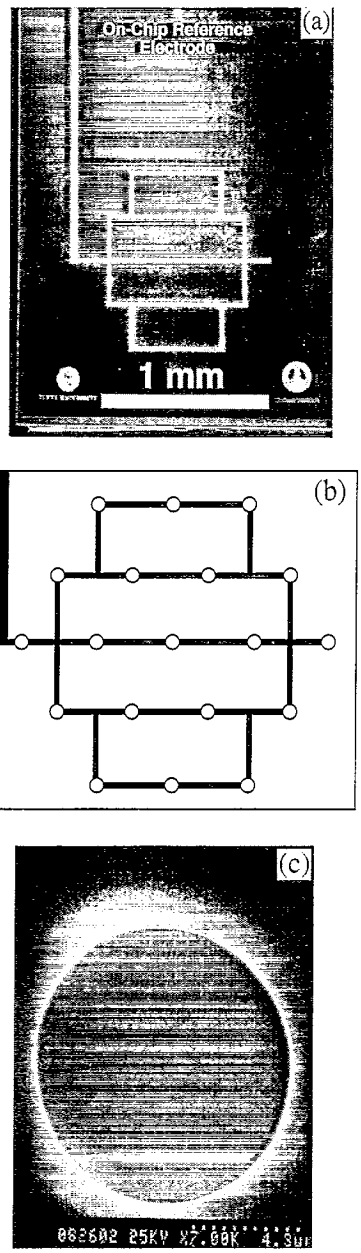

Fig. 4. (a) Overall SEM view of a 'skeleton' microelectrode array. Microelectrode sites are located at 300 μm intervals on the central 'skeleton' of iridium. A gold interconnect trace can be seen running from top to bottom on the left-hand side of the image. (b) Diagram showing locations of the individual microelectrodes. (c) Close-up view of an individual 10 μm diameter microelectrode site.

erence electrode into the sample. All potentials were measured relative to this counter electrode (approximately +220 mV versus SCE), with the exception of mercury deposition, as described below.

Mercury deposition was carried out using a solution containing 8×10^{-3} M Hg(II) (from 99.9995% $Hg_2(NO_3)_2$ from ALFA-Johnson Matthey, Ward Hill, MA) in 0.1 M $HClO_4$ at a potential of −0.2 V versus a sodium-saturated calomel reference electrode. The amount of charge was controlled by timing the Hg depositions, and the amount of Hg deposited could readily be varied from a thin film to almost a sphere. For maximal ruggedness and stability, a hemispherical or spherical segment geometry was used.

For the 19-element microelectrode array described above, a total charge of 260 μC resulted in hemispherical Hg coverage. Once the Hg was deposited, the microelectrode arrays were rinsed with 18 MΩ deionized water and used for experiments.

Metal ion test solutions were prepared from 99.9995% $Cu(NO_3)_2$, $Cd(NO_3)_2$, $Zn(NO_3)_2$ (ALFA-Johnson Matthey, Ward Hill, MA), and $Pb(NO_3)_2$ (Aldrich). Acetate buffer solutions were prepared with 99.99+% ammonium acetate and acetic acid, and the pH adjusted to 4.5 by addition of $HClO_4$ (Aldrich).

5. Results

In order to demonstrate the analytical utility of the Ir microelectrode arrays, they were used for SWASV testing of various solutions. Deionized water containing 2 mM acetate buffer was used for the initial tests, with successive additions of Cd^{2+}, Pb^{2+}, Cu^{2+}, and Zn^{2+} in concentrations ranging from 1 to 40 ppm for each metal. The test solution was neither deoxygenated nor stirred, and deposition was followed immediately by anodic stripping (no equilibrium period). SWASV was carried out with $E_{sw}=25$ mV, $\Delta E_s=5$ mV, $f=120$ Hz, with a deposition potential of −1400 mV for 260 s. The resulting square-wave voltammograms (with baseline subtraction) are shown for 1, 2, 3, 4, and 5 ppb concentrations in Fig. 5.

The detected peaks for each metal were sharp and well defined, and plots of peak current versus concentration yielded straight lines with intercepts at zero with the exception of Cu and Zn, which showed a slight curvature above 10 ppb. This is due to the fact

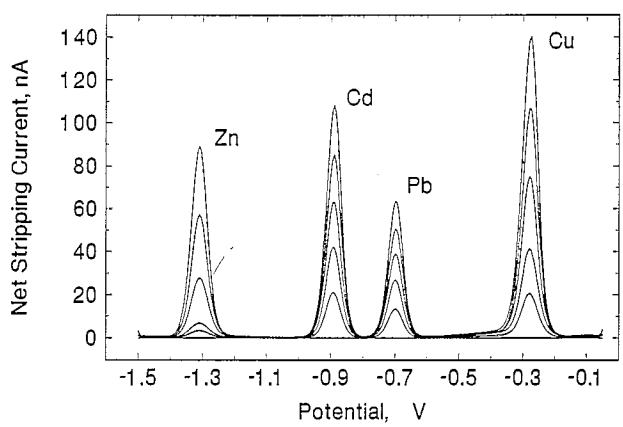

Fig. 5. Square-wave voltammograms for successive additions of Cd^{2+}, Pb^{2+}, Cu^{2+}, and Zn^{2+} to deionized water containing 2 mM acetate buffer to yield concentrations of 1, 2, 3, 4, and 5 ppb for each metal. This solution was neither deoxygenated nor stirred during analysis, and stripping was begun immediately following the preconcentration step. SWASV was carried out with $E_{sw}=25$ mV, $\Delta E_s=5$ mV, $f=120$ Hz, with a predeposition potential of −1400 mV for 260 s.

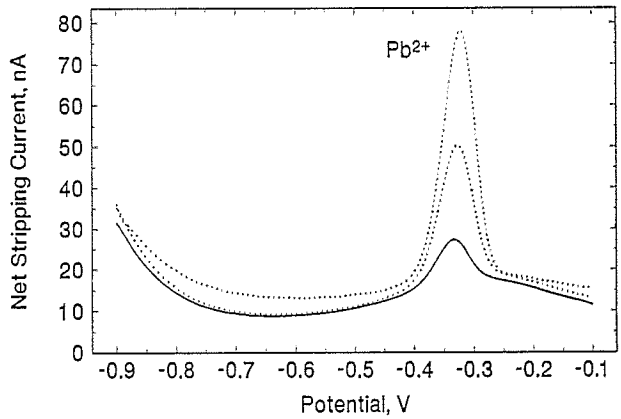

Fig. 6. Square-wave voltammogram for tap water (Stanford Sample D) acidified to pH 2 (HNO_3) and with standard additions of 5 and 10 ppb of lead, which indicate a sample concentration of 3.0 ± 0.3 ppb Pb^{2+}. The solution was neither deoxygenated nor stirred during the analysis and no equilibration period was allowed between the deposition and stripping steps. SWASV was carried out with $E_{sw}=25$ mV, $\Delta E_s=5$ mV, $f=120$ Hz, with a predeposition potential of -900 mV (vs. 3 M Ag/AgCl) for 180 s.

that Cu and Zn form an intermetallic compound when they are both simultaneously reduced into the Hg at higher concentrations.

To provide an example of use of the sensor with a sample of local potable water, SWASV testing was carried out on tap water acidified to pH 2 with HNO_3. The results, also showing those for standard additions of 5 and 10 ppb of lead, are shown in Fig. 6. The results indicate a sample concentration of 3.0 ± 0.3 ppb Pb^{2+}. The solution was neither deoxygenated nor stirred during the analysis and no equilibration period was allowed between the deposition and stripping steps. SWASV was carried out with $E_{sw}=25$ mV, $\Delta E_s=5$ mV, $f=120$ Hz, with a predeposition potential of -900 mV (versus 3 M Ag/AgCl) for 180 s.

6. Discussion and conclusions

We have demonstrated a versatile microelectrode array transducer for the detection of heavy metal ions with sensitivities down to parts per billion in aqueous media. The devices are fabricated using techniques available in most integrated-circuit fabrication laboratories. Since these processes are inherently batch oriented, the devices can readily be mass-produced.

A long-term goal of this work is to build not only stand-alone microelectrode arrays for analytical/clinical chemistry applications, but also to integrate them with control circuitry to form complete compact electroanalytical instruments (for environmental or process monitoring, clinical analysis or consumer use).

In order to realize such systems, we have undertaken the development of a single-chip potentiostat that can be directly interfaced to an inexpensive microcontroller, with data transmitted from there to a personal computer in digital form [14]. It is hoped that such systems can be realized in the near term, with all of the active elements contained within a volume on the order of one cubic centimeter (naturally, application-specific packaging would define the external form factor).

Present efforts are focused on further characterization of the sensor (particularly in terms of determining detection limits and verifying long-term repeatability), optimization of the design and packaging, and the realization of the integrated system version of the sensor described above.

Acknowledgements

The authors would like to thank Pamela Hallock for her help with the characterization of the devices and Dr Nadim Maluf for his help with the layout of the printed circuit boards. Initial development of the micromachining aspects of this work was supported by Stanford Center for Integrated Systems (CIS) Seed and Research Thrust Grants, the US Department of Veterans Affairs, and funds from the Robert N. Noyce Family Faculty Scholar Chair (Kovacs). On-going efforts are funded by grants from the US Environmental Protection Agency, the Stanford Center for Integrated Systems, the Northeast Hazardous Substance Research Center, EG&G Princeton Applied Research Corporation, and the National Science Foundation (CHE-9256871).

References

[1] J. Wang, *Stripping Analysis*, VCH, Deerfield Beach, FL, 1985.
[2] J.G. Osteryoung and R.A. Osteryoung, Square wave voltammetry, *Anal. Chem., 57* (1985) 101A–105A.
[3] A.S. Baranski, Rapid anodic stripping analysis with ultramicroelectrodes, *Anal. Chem., 59* (1987) 662–666.
[4] S.P. Kounaves and J. Buffle, Deposition and stripping properties of mercury on iridium microelectrodes, *J. Electrochem. Soc., 133* (1986) 2495–2498.
[5] C. Guminski and Z. Galus, in C. Hirayama, C. Guminski and Z. Galus (eds.), *Solubility Data Series — Metals in Mercury*, Vol. 25, Pergamon Press, Oxford, 1986.
[6] S.P. Kounaves, The stability of micro mercury hemispheres deposited on iridium substrates, *J. Electroanal. Chem.*, (1993) in press.
[7] S.P. Kounaves and W. Deng, An iridium-based ultramicroelectrode — fabrication and characterization, *J. Electroanal. Chem., 301* (1991) 77–85.
[8] K. Aoki and J. Osteryoung, Diffusion controlled current at a finite disk electrode, *J. Electroanal. Chem., 125* (1981) 315–320.
[9] W.L. Caudill, J.O. Howell and R.M. Wightman, Flow-rate independent amperometric cell, *Anal. Chem., 54* (1982) 2532–2535.
[10] T. Hepel and J. Osteryoung, Electrochemical characterization of electrodes with submicrometer dimensions, *J. Electrochem. Soc., 133* (1986) 752–757.

[11] G.T.A. Kovacs, C.W. Storment and J.M. Rosen, Regeneration microelectrode array for peripheral nerve recording and stimulation, *IEEE Trans. Biomed. Eng., BME-39* (1992) 893–902.
[12] S.J. Tanghe, K. Najafi and K.D. Wise, A planar IrO multichannel stimulating electrode for use in neural prostheses, *Sensors and Actuators, B1* (1990) 464–467.
[13] S.P. Kounaves, W. Deng, P.R. Hallock, G.T.A. Kovacs and C.W. Storment, A microlithographically fabricated iridium-based mercury ultramicroelectrode array and its application to SWASV analysis of metal ions in natural waters, *Anal. Chem., 66* (1994) 418–423.
[14] R.J. Reay, S.P. Kounaves and G.T.A. Kovacs, An integrated CMOS potentiostat for miniaturized electroanalytical instrumentation, accepted for publication, *Proc. 1994 IEEE Int. Solid-State Circuits Conf., San Francisco, CA, Feb. 16–18, 1994*, pp. 162–163.

Biographies

Gregory T.A. Kovacs was born in Vancouver, British Columbia, in 1961. He received the B.A.Sc. degree in electrical engineering from the University of British Columbia, Vancouver, B.C., in 1984, the M.S. degree in bioengineering from the University of California, Berkeley, in 1985, the Ph.D. degree in electrical engineering from Stanford University in 1990, and the M.D. degree from Stanford University in 1992.

His industrial experience includes the design of high-speed data-acquisition systems, a precision pulsed-electroplating system for GaAs device fabrication, patent law consulting, and the co-founding of three electronics companies. In 1991, he joined Stanford University as assistant professor of electrical engineering. His present research areas include neural/electronic interfaces, solid-state sensors and actuators, micromachining, integrated circuit fabrication, medical instruments, and biotechnology. He holds the Robert N. Noyce Family Faculty Scholar Chair and a National Science Foundation Young Investigator Award.

Christopher W. Storment was born in Burbank, California, in 1957. He received the B.S. degree in chemistry from the University of California, Riverside, in 1980, and the M.S. degree in material sciences from the University of Southern California, Los Angeles, in 1987.

From 1980 to 1987, he was employed at the Hughes Aircraft Torrance Research Center and the TRW Advanced Microwave Circuits Department, working on process development for GaAs digital and analog microwave circuits. Between 1987 and mid-1993, he worked at the Palo Alto Veterans Administration Rehabilitation Research and Development Center developing fabrication techniques for use in the neural interface project (at Stanford). He recently joined the Department of Electrical Engineering at Stanford University, where he is a research and development engineer. He is active in co-advising students on several other solid-state transducer projects in Dr. Kovacs' laboratory at Stanford University.

Samuel P. Kounaves was born in Anaconda, Montana, in 1948. He received B.S. and M.S. degrees in chemistry from California State University – San Diego in 1975 and 1978, respectively, and the Ph.D. degree from the Université de Genève, Switzerland, in 1985. After post-doctoral studies at S.U.N.Y. Buffalo (1985–86) and Harvard Medical School (1986–88), he joined the faculty at Tufts University, where he currently holds an appointment as assistant professor in the Chemistry Department.

His research interests include electroanalytical chemistry and its applications to environmental monitoring, multi-element and immobilized enzyme sensors, ultramicroelectrode arrays, and the electrochemistry of metal and alloy film deposition using heteropolymetallic complexes.